Los Alamos National Laboratory is operated by the University of California for the United States Department of Energy under contract W-7405-ENG-36

TITLE THE SPATIAL DEPENDENCE OF SPIN AND CHARGE CORRELATIONS IN A ONE-DIMENSIONAL, SINGLE IMPURITY, ANDERSON MODEL

LA-UR--86-3745

DE87 002927

AUTHOR(S) James E. Gubernatis

SUBMITTED TO Taniguchi Symposium on Quantum Monte Carlo, Shizuoka, Japan, November 13-18, 1986.

DISCLAIMER

Los Alamos Los Alamos National Laboratory
Los Alamos, New Mexico 87545

FORM NO 836 R4
ST NO 2629 5/81

The Spatial Dependence of Spin and Charge Correlations in a One-Dimensional, Single Impurity, Anderson Model

J. E. Gubernatis
Theoretical Division, Los Alamos National Laboratory
Los Alamos, NM 87545, USA

1. Introduction

Recent advances in Monte Carlo algorithms for systems of interacting electrons have made possible the detailed study of the spatial dependence of spin and charge correlations in the Anderson single impurity model. The hamiltonian for this model [1]

$$H = \sum_{ks} \varepsilon_k n_{ks} + \sum_{k} (V_{kd} c^{+}_{ks} c_{ds} + V^{*}_{dk} c^{+}_{ds} c_{ks}) + \varepsilon_d \sum_{s} n_{ds} + U n_{d\uparrow} n_{d\downarrow} \qquad (1)$$

has a non-degenerate impurity state with energy ε_d hybridized with strength V_{kd} to energy states ε_k of some conduction band. In addition it has a Coulomb interaction U between electrons with oppositely paired spins that try to occupy the impurity state.

As a function of interaction parameters and temperature, the model exhibits a variety of interesting many-body phenomena [2,3]. One of these phenomena is the existence of a local magnet moment at the impurity and the compensation of this moment by a spin cloud that leaves the system in a singlet state as $T \to 0$. Prior to recent Monte Carlo simulations the structure of this spin compensation cloud was accessible only through perturbative theories that lead to somewhat controversial or incomplete results [4].

In investigations of the spatial dependence of this spin compensation, the first [5] of a series of Monte Carlo studies found RKKY and Friedel-like oscillations with a strong negative (antiferromagnetic) correlation between electrons at the impurity site and those at the lattice site with which it interacts. With a wave number of $2k_F$, these oscillations alternated in sign and decreased in amplitude as the distance from the impurity site increased. The principal limitation of this study was its inability to probe temperatures well below the Kondo temperature T_K. Subsequently proposed was another approach [6] that reached these low temperatures, at the expense of losing the information about the spatial dependence of correlations, and had the additional advantage of embedding the impurity in an infinite system. The most recent study [7] showed within this new approach how to recover the spatial dependence and presented low temperature results that had several surprising features.

Perhaps the most surprising feature was the possible extension of the spin compensation cloud to distances beyond the apparent natural length v_F/T_K, where v_F is the fermi velocity. If the compensation in physical systems is this long-ranged, then the single impurity results would most likely have applicability only to very dilute alloys, and the quantitative comparison between theory and experiment, notwithstanding the neglect of orbital degeneracy, would be difficult. Along with a closer examination of this possible long-ranged correlation, several other interesting features were found that await a clearer understanding. These novel features included a non-monotonic variation of the lattice site to impurity site spin correlation as a function of the Coulomb interaction.

The principal purpose of this short note is to present corroborative results for most of these features. A secondary purpose is to highlight several additional systematic, but small, features that become apparent by going to lower temperatures. Whereas the original study assumed the computationally convenient model of the conduction band as a broad flat density of states and a free-electron dispersion, here we assume a one-dimensional, tight-binding band

$$\varepsilon_k = -2 \cos k \quad . \tag{2}$$

In the next section we summarize the Monte Carlo procedure. Then in the third section we present the results of our calculation. In the fourth and final section we summarize our findings and comment on further applications of the procedure to the study of quantum many body phenomena.

2. Procedure

The procedure we use is that of [7] and starts with a discrete, path integral approach [8] to the evaluation of the partition function in which the temperature axis is divided into L steps of size $\tau = \beta/L$. At each step the Trotter approximation is made

$$e^{-\tau H} \simeq e^{-\tau H_0}\, e^{-\tau H_I} \tag{3}$$

and then the interaction term in the hamiltonian is eliminated by introducing auxiliary Ising variables σ_ℓ [9], one for each step,

$$e^{-\tau\frac{U}{2}(n_{d\uparrow}-n_{d\downarrow})^2} = \frac{1}{2} \sum_{\sigma_\ell=\pm 1} e^{-\tau J\sigma_\ell(n_{d\uparrow}-n_{d\downarrow})}$$

with $\cosh \tau J = \exp(-\tau U/2)$. After this transformation the partition function becomes

$$Z = \mathrm{Tr}_\sigma \exp(-\sum_s \mathrm{Tr}\, \ell n\, g^s[\sigma]) \tag{4}$$

where the matrix $g^s[\sigma]$ is the equal-time thermodynamic Green's function whose elements are defined by

$$g^s_{ij}(\ell\ell') = \langle T c^\dagger_{is}(\ell)\, c_{js}(\ell')\rangle \tag{5}$$

The Monte Carlo part of the procedure performs the trace over the σ configurations and consists of successively flipping the σ_ℓ and accepting or rejecting the flip on the basis of whether the quantity $R/(1+R)$ is greater than or less than a random number between 0 and 1 [5]. R is the ratio of the partition function for the new configuration to partition function for the old configuration and equals $R_\uparrow R_\downarrow$ with

$$R_s = (1 + (1 - g^s_{dd}(\ell\ell))(\Delta^s_d(\ell) - 1) \tag{6}$$

where $\Delta^s_d(\ell)$ is the change in energy caused by the change in the field.

As pointed out by Hirsch and Fye [6], within the Trotter approximation there is a general relation between the spatial and time elements of the Green's functions for two σ configurations differing at time step ℓ''. For each component of electron spin

$$g'_{ij}(\ell\ell') = g_{ij}(\ell\ell') + (\delta_{id}\delta_{\ell\ell''} - g_{id}(\ell\ell'')) \times (\Delta_d(\ell'') - 1)\, g'_{dj}(\ell''\ell') \tag{7}$$

In our Monte Carlo procedure we use this relation for three different purposes [7]. First to initialize the calculation, we chose the σ_ℓ randomly. Having computed the $g_{dd}(\ell\ell')$ for the non-interacting problem, we use (7) iteratively to turn on the σ_ℓ one at a time at each step of the interation to obtain $g'_{dd}(\ell\ell')$ for the complete configuration: With the unperturbed $g_{dd}(\ell\ell')$ we use (7) to find $g'_{dd}(\ell\ell')$ for system with just σ_1. We then use this a $g_{dd}(\ell\ell')$ on the right side of (7) to find $g'_{dd}(\ell\ell')$ for a system with σ_1 and σ_2. We continue turning on the spins this way until we construct the Green's function for all the spin variables. With the $g_{dd}(\ell\ell')$ we can begin the Monte Carlo steps and evaluate (6). If we accept the flip, we use (7) again to compute the $g_{dd}(\ell\ell)$ for the new configuration [10],

$$g'_{dd}(\ell\ell) = g_{dd}(\ell\ell) - \frac{(g_{dd}(\ell\ell)-1)(\Delta_d(\ell)-1)g_{dd}(\ell\ell)}{1+(1-g_{dd}(\ell\ell))(\Delta_d(\ell)-1)} \tag{8}$$

The third use of (5) is to recover the spatial information about the Green's functions, since only the impurity elements $g_{dd}(\ell\ell')$ are the natural product from the Monte Carlo steps. Here we are interested in determining $g_{dj}(LL)$, $g_{id}(LL)$ and $g_{ij}(LL)$. From (7) we have

$$g'_{dd}(L\ell') = g_{dd}(L\ell') + (\delta_{L\ell''} - g_{dd}(L\ell''))(\Delta_d(\ell'') - 1)g'_{dd}(\ell''\ell') \tag{9a}$$

$$g'_{dj}(L\ell') = g_{dj}(L\ell') + (\delta_{L\ell''} - g_{dd}(L\ell''))(\Delta_d(\ell'') - 1)g'_{dj}(\ell''\ell') \tag{9b}$$

where j is a lattice site. We use (9) the same way as we used (7) to get $g_{dd}(\ell\ell')$: Starting with the non-interacting Green's functions $g_{dd}(L\ell')$ and $g_{dj}(L\ell')$, we iterate (9) and at each step turn-on a new spin until $g'_{dj}(L\ell')$ for the given configuration is constructed.

To find $g_{dj}(LL)$ and $g_{ij}(LL)$, we use a similar procedure except we rewrite (7) by interchanging the labels of the old and new configurations

$$g'_{ij}(\ell\ell') = g_{ij}(\ell\ell') - (\delta_{id}\delta_{\ell\ell''} - g'_{id}(\ell\ell''))$$

$$\times (\Delta_d^{-1}(\ell'') - 1)\, g_{dj}(\ell''\ell') \tag{10}$$

This leads to

$$g'_{id}(L\ell) = g_{id}(L\ell) + g'_{dd}(L\ell'')(\Delta_d^{-1}(\ell'')-1)g_{dd}(\ell''\ell) \tag{11a}$$

$$g'_{ij}(L\ell) = g_{ij}(L\ell) + g'_{id}(L\ell'')(\Delta_d^{-1}(\ell'')-1)g_{dd}(\ell''\ell) \tag{11b}$$

with i and j being lattice sites. Hence starting with $g'_{dd}(L\ell)$ and $g'_{id}(L\ell)$ found from equation (8) and with the non-interacting $g_{dj}(L\ell)$ and $g_{ij}(L\ell)$, we use the iteration-turn-on technique to find $g'_{dj}(L\ell)$ and $g'_{ij}(L\ell)$. An important point to appreciate about the procedures just outlined is we can start with the Green's function for an infinite, non-interacting system and obtain the Green's function of the infinite interacting system at a finite number of states of our choosing.

With the Green's functions one can compute the thermodynamics quantities of interest. In this paper we are mainly interested in the impurity susceptibility

$$T\chi_d = \int_0^\beta d\tau \langle \sigma_d(\tau)\sigma_d(L)\rangle \tag{12a}$$

the impurity moment

$$S_d = \langle (\sigma_d(L))^2 \rangle \tag{12b}$$

and the correlation between the spin at the impurity and the spin at lattice sites

$$S(i) = \langle \sigma_d(L)\sigma_i(L)\rangle \tag{12c}$$

where $\sigma_d = n_{d\uparrow} - n_{d\downarrow}$ and $\sigma_i = n_{i\uparrow} - n_{i\downarrow}$.

The averages over the products of these spins are related to the Green's functions by use of Wick's theorem. The application of Wick's theorem simplifies somewhat because the introduction of the auxiliary fields leaves the Green's function in a representation block-diagonal in the electron spin. As an example, we can express (12c) as

$$S(i) = \langle (g^{\uparrow}_{dd}-g^{\downarrow}_{dd})(g^{\uparrow}_{ii}-g^{\downarrow}_{ii})\rangle - \langle g^{\uparrow}_{id}g^{\uparrow}_{di}+g^{\downarrow}_{id}g^{\downarrow}_{di}\rangle \tag{13}$$

where the average is over σ configurations.

We will also present results showing the nature of charge compensation. Defining $n_d = n_{d\uparrow}+n_{d\downarrow}$ and $n_i = n_{i\uparrow}+n_{i\downarrow}$, we have the following quantities in analogy to equation (12):

$$T\Pi_d = \int_0^\beta d\tau \langle n_d(\tau)n_d(L)\rangle \tag{14a}$$

$$C_d = \langle (n_d(L))^2 \rangle \tag{14b}$$

$$C(i) = \langle n_d(L)\, n_i(L)\rangle - \langle n_d(L)\rangle\langle n_i(L)\rangle \qquad (14c)$$

To compute the averages over the σ configurations, we generate 1024 configurations to equilibrate the system, and then generate an additional 5120 configurations from which we compute the averages. These additional configurations are split into 20 groups on which we do coarse grain-averaging and obtain estimates of statistical error [11]. In general, our statistical error is no more than several percent and is larger than error we make using the Trotter approximation. This latter error limits the accuracy of our Green's functions to about the fourth decimal place and is noticeable only at low temperatures when some of our measured quantities become comparably sized.

3. Results

Here we report results for the particle-hole symmetric case where $\varepsilon_d = -U/2$ and $\langle n_d\rangle = 1$. For all our calculations $\tau = 0.25$ and the fermi energy $\mu = 0$. At $T = U = 0$ this choice of μ corresponds to a half-filled band. We considered cases for $V = 1$ and $1/\sqrt{2}$, so that at $U = 0$ the full width of the impurity resonance, $2\Gamma = \pi\rho_F V^2$, is 1 and 1/2. For $\Gamma = 1/2$, we computed cases for $U = 1/4$, 1/2, 1, 2, 3, and 4; for $\Gamma = 1/4$, $U = 0$, 1, 2, 4. A summary of our results will now be given.

Three-dimensional plots of the spatial and temperature dependence of the spin-correlation (12c) and charge correlation (14c) functions for $U = 0$ and 2 are shown in Fig. 1. Apart from the overall scale, the two U cases are remarkably similar: There is a strong negative correlation between the impurity and the central lattice site, and the amplitude decreases as it spreads to other sites in the lattice. For $\beta < 10$ only a few nearest neighbors are correlated to the impurity, while for $\beta < 10$, the correlation spreads more rapidly outward and the amplitudes at the impurity and the closest neighbors are becoming somewhat independent of β.

To see specific effects of $U \neq 0$ on these correlations, we have to take a closer look at their U and β dependence. We find the principal effect of $U \neq 0$ is the induction of ferromagnetic spin correlations at the sites between the antiferromagnetically correlated sites. These correlations increase with increasing U. On the other hand, the correlations at the antiferromagnetic sites are often supressed if U becomes large enough. The number of sites at which this suppression occurs is reduced to just the impurity site if β is well above β_K. The importance of being at low temperatures to reduce the suppression of the antiferromagnetic correlations was underscored by comparing the results for $\Gamma = 1/2$ and 1/4. For most our U values the lower Γ pushes β_K outside the range of our simulation and the suppression then occurs at most of antiferromagnetic sites studied.

The Coulomb interaction also induces a negative charge correlation at sites where the ferromagnetic spin correlation was induced. These correlations show a non-monotonic variation with U -- first increasing, then decreasing. The correlations at the antiferromagnetically correlated spin sites are suppressed as U is increased. We note that our charge correlation function (14c) differs from that discussed in [7] since at each site we subtract from $\langle n_d n_i\rangle$ the decorrelated value $\langle n_d\rangle\langle n_i\rangle$ for that site as opposed to the decorrelated valued for a site infinitely far away. The definition also allows (16), defined below, to express charge conversation

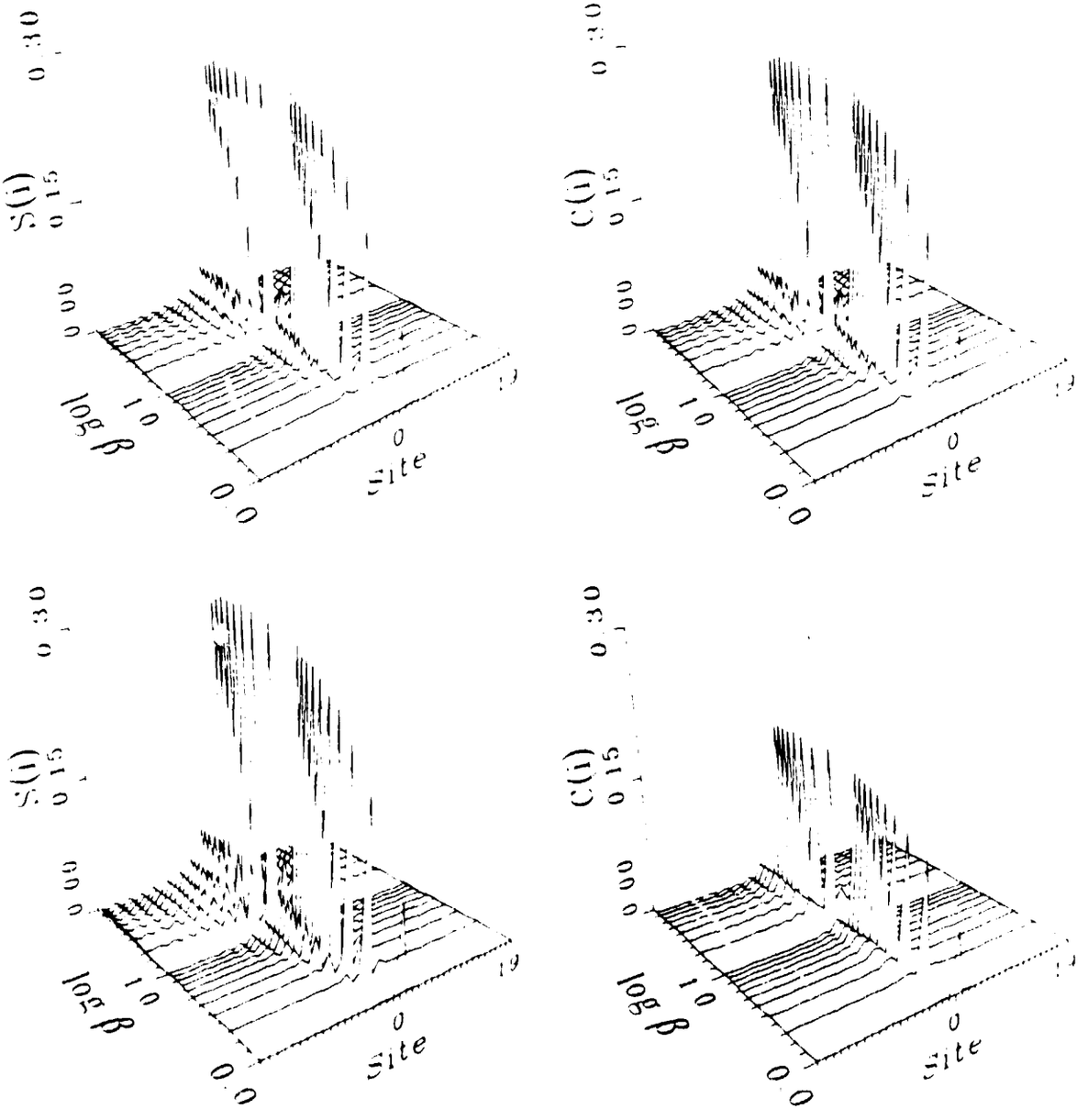

Fig 1 On the top row is the spin and charge correlation functions for V = 1 and U = 0 as a function of position and β. On the bottom row are the same correlation functions but with U = 2.

at T = 0 as $T \Pi_d \to 1$ for the symmetric model and makes S(i) = C(i) for U = 0 as can be seen from Fig. 1. Hence the U = 2 plots in this figure dramatizes the different consequences a non-zero interaction has on the spin and charge correlations. Overall increasing U enhances spin correlations and suppresses charge correlations, but specific details show a range of behavior. Some of the behavior just summarized is illustrated in Fig. 2. We point out that most of the effects are quite small.

For a given U, the effect of increasing β is to increase the antiferromagnetic spin correlations. At large β the rate of increase slows to the

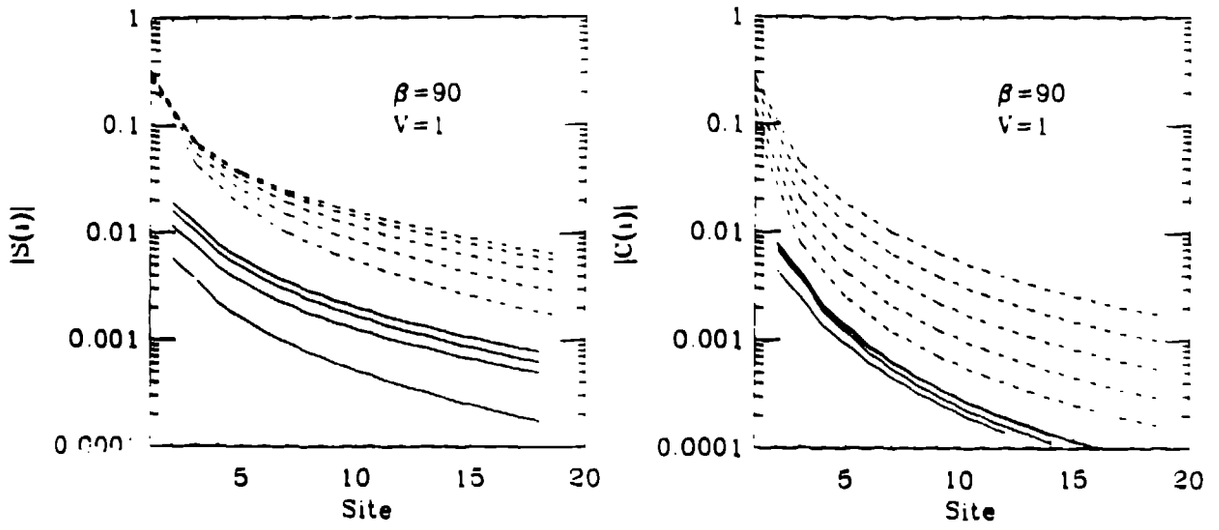

Fig. 2 Variation of the spin and charge correlations as a function of position and U. The solid lines connect the values of the function at odd lattice sites, which include the impurity site, and the dashed lines, the even sites. For the spin correlation the upper line of each type corresponds to U = 4. For the charge correlations, the lowest solid line corresponds to U = 0, while lowest dashed line corresponds to U = 0. Plotted are cases for U = 0, 1, 2, 3, and 4.

point where in some cases the correlations at the impurity and several nearby sites appear to be saturating. On the other hand, the ferromagnetic spin correlations at first increase and then become suppressed as β is increased. Only for β above β_K do the trends become most apparent. The charge correlations behave similarly. Some of this behavior is depicted in Fig. 3. Again the effects are generally small.

In [7] the following sum rule, representing the spin compensation in the same spirit as the Clogston-Anderson compensation theorem [12], was found to hold

$$\sum_i \langle \sigma_d(L)\, \sigma_i(L) \rangle = T\chi_d - \langle \sigma_d(L)^2 \rangle \qquad (15)$$

We also find this relation to hold, as well as the analogous relation for charge compensation

$$\sum_i \langle n_d(L)\, n_i(L) \rangle = T\,\Pi_d - \langle n_d(L)^2 \rangle \qquad (16)$$

At low temperatures we find the correlation functions to decay as $i^{-\alpha}$. For the spin compensation sum rule to hold, we had to correct the sum over $1 \leq i \leq |20|$ by fitting the ferromagnetic and antiferromagnetic peaks separately to the form $A\, i^{-\alpha}$ and then summing the resulting expression over a large number of additional sites. For charge compensation this procedure, for all practicle purposes, was unnecessary. At high temperatures we found an exponential decay instead of the power law behavior. These functional dependences on i

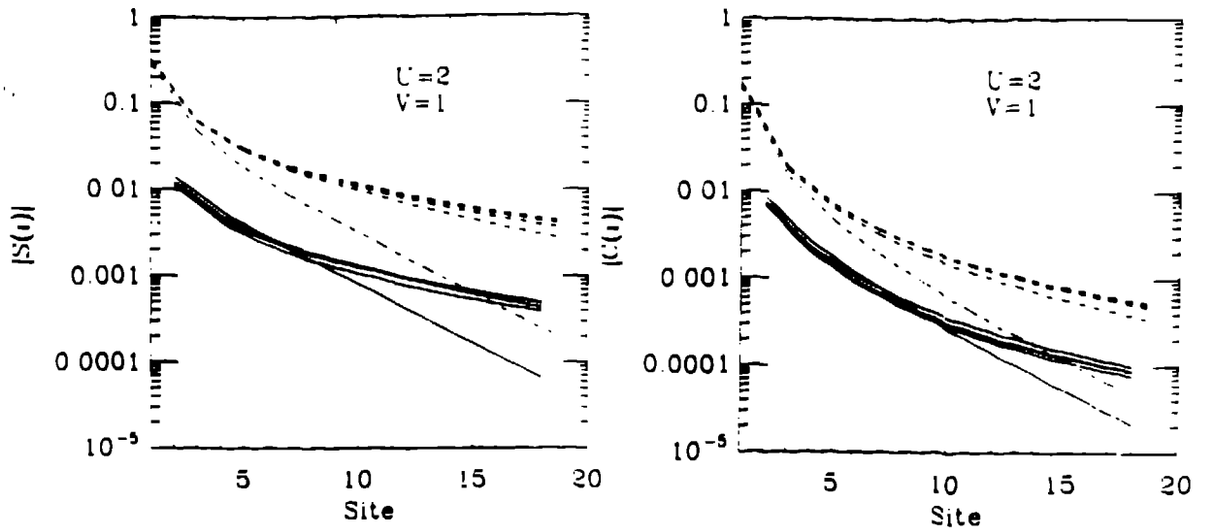

Fig. 3 Variation of the spin and charge correlations as a function of position and β. The line types are described in Fig. 2. In both figures the lowest lying solid and dashed lines, which for the most part are straight lines, corresonds to β = 10. Plotted are the cases for β = 10, 30, 50, 70, and 90.

were also found for the U = 0 case. The different behaviors are illustrated in Fig. 4.

4. Summary

We summarized the results of a series of quantum Monte Carlo calculations of the spatial dependence of spin and charge correlations in a one-dimensional, single impurity, symmetric Anderson model. We corroborated several features of [7], and because we achieved lower temperatures, we were able to identify several additional unusual features in the behavior of the correlations as functions of U and β. We also showed the existence of a charge compensation sum rule and found a power law decay of the correlations at low temperatures.

To corroborate some of the low temperature behavior discussed here, carrying the calculation to lower temperatures would be desirable but unfortunately would also be costly. The procedure described scales in computer time as L^3, and on a Cray X-MP/48 for the number sweeps described, the 360 steps to achieve β = 90 took around 145 minutes. The vectorization achieved on a Cray computer reduces power in L^3 to something slightly less than 3. Although slightly less, the reduction in time is noticeable at low temperatures. Not withstanding this, doubling β would be expensive to do and most likely be just partly helpful.

Within the parameter and temperature range discussed here, there are other interesting aspects of the Anderson model that can be explored. For the asymmetric Anderson model, valence fluctuation phenomena occur and can easily be studied and has been observed with the same program used for the symmetric model [13]. Orbital degeneracy effects and magnetic fields can be added to the model, and as pointed out elsewhere [6,7], more than one

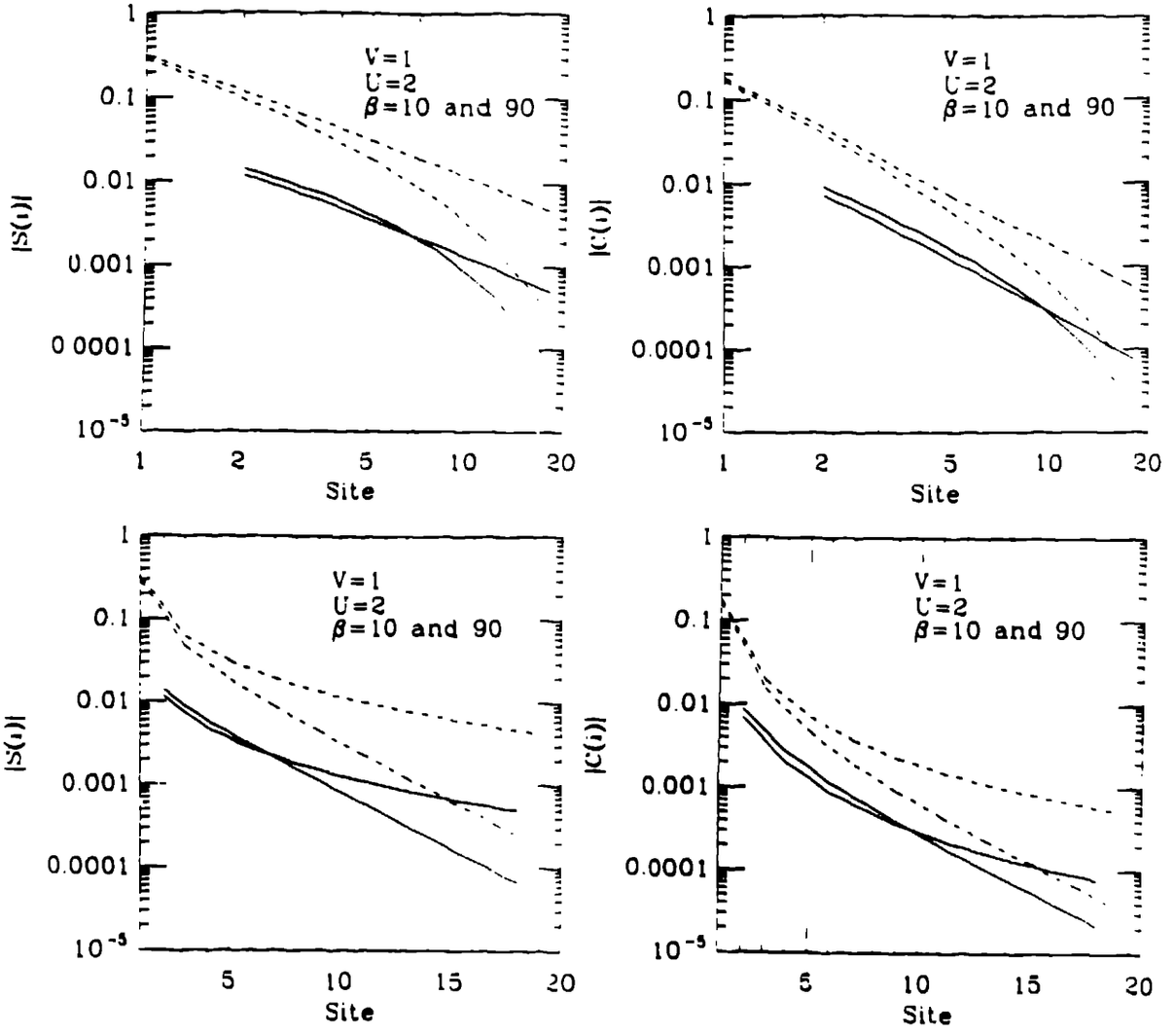

Fig. 4 The functional form of the spatial dependence of the spin and charge correlations at high and lowest temperatures. In the top row the straight lines, indicative of a exponential, are for β = 10; on the bottom row the straight lines, indicative of a power law, β = 90. The line types are defined in Fig. 2.

impurity can be treated and realistic band structures can be used. Some of this work is currently underway.

5. Acknowledgements

Support for the calculations was provided by the Center for Materials Science at the Los Alamos National Laboratory.

6. References

1. P. W. Anderson: Phys. Rev. 124, 41 (1965).
2. F. D. M. Haldane: Phys. Rev. Lett. 40, 416 (1978).
3. H. R. Krishna-Murthy, J. W. Wilkins and K. G. Wilkins: Phys. Rev. B 21, 1003 (1980); 21, 1044 (1980).

4. For example, see G. Grüner and A. Zawadowski: Rep. Prog. Phys. 37, 1497 (1974). Recently, a new approach combining perturbative scaling and non-perturbative renormalization-group methods has been applied to a related problem by K. Chen, C. Jayaprakresh and H. R. Krishna-Murthy in the preprint "Spatial Correlations around a Kondo Impurity."
5. J. E. Gubernatis, T. C. Olson, D. J. Scalapino, and R. L. Sugar: J. Stat. Phys. 43, 831 (1986); J. E. Gubernatis, Los Alamos Technical Report LA-UR-86-2748.
6. J. E. Hirsch and R. M. Fye: Phys. Rev. Lett. 56, 2521 (1986).
7. J. E. Gubernatis, J. E. Hirsch, and D. J. Scalapino: Los Alamos Technical Report LA-UR-86-3510.
8. R. Blankenbecler, D. J. Scalapino, and R. L. Sugar: Phys. Rev. D 24, 2278 (1981).
9. J. E. Hirsch: Phys. Rev. B 28, 4059 (1983).
10. Historically, this equation was first derived in Ref. 8 and is the basis for other finite temperature quantum Monte Carlo methods for the simulations of fermion systems. For examples of prior use, see Ref. 5 or 9.
11. K. Binder: in Applications of the Monte Carlo Method in Statistical Mechanics, ed. by K. Binder. Topics in Current Physics, Vol. 36, (Springer, New York, 1984) p. 1.
12. A. M. Clogston and P. W. Anderson: Bull. Am. Phys. Soc. 6, 124 (1961).
13. J. E. Gubernatis, unpublished.